Supplementary Information

Magneto-optical hyperthermia agents based on probiotic bacteria loaded with magnetic and gold nanoparticles

Víctor Garcés,[a] Ana González,[a] Natividad Gálvez,[a] José M. Delgado-López,[a] Jose J. Calvino,[b] Susana Trasobares,[b] Yilian Fernández-Afonso,[c] Lucía Gutiérrez,[c,*] and José M. Dominguez-Vera,[a,*]

[*] Corresponding authors: J.M. Domínguez-Vera and L. Gutiérrez

[a] Departamento de Química Inorgánica and Instituto de Biotecnología
Universidad de Granada,
18071 Granada, Spain
E-mail: josema@ugr.es

[b] Departamento Ciencia de Materiales e Ingeniería Metalúrgica y Química Inorgánica
Universidad de Cádiz
11510 Cádiz, Spain

[c] Departamento de Química Analítica, Instituto de Nanociencia y Materiales de Aragón (INMA)
CSIC- Universidad de Zaragoza and CIBER-BBN
50018 Zaragoza, Spain
E-mail: lu@unizar.es

1. MNP characterization and stability at pH 2.5

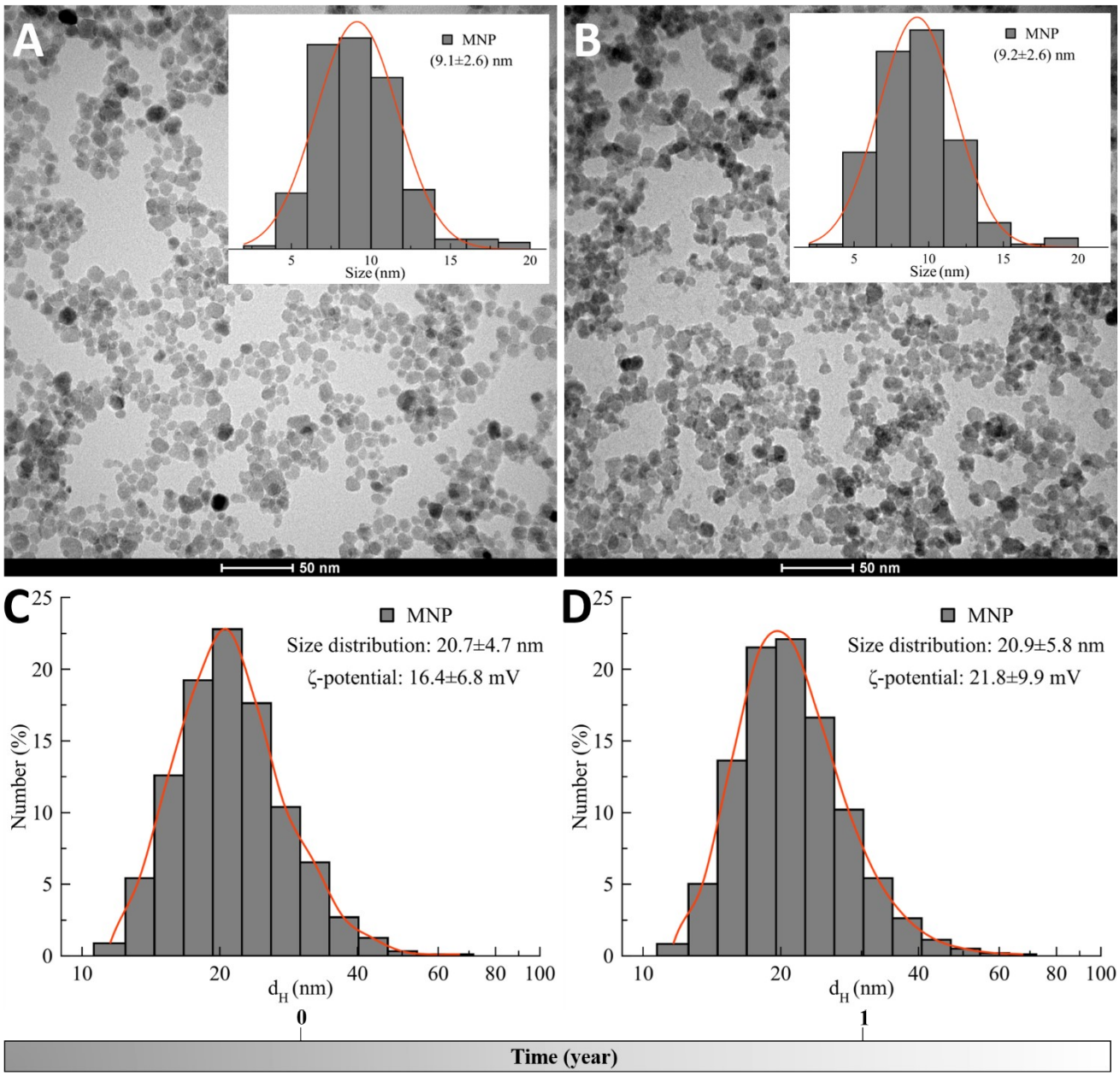

Figure SI1. TEM images of: A) Maghemite nanoparticles (MNP) immediately after their synthesis (inset, size distribution by TEM); B) MNP one year after the synthesis (inset, size distribution by TEM). C and D) DLS particle size distributions (hydrodynamic diameter, d_H) and ζ-potentials of: C) MNP immediately after synthesis and D) MNP one year after the synthesis. A time scale is depicted at the bottom.

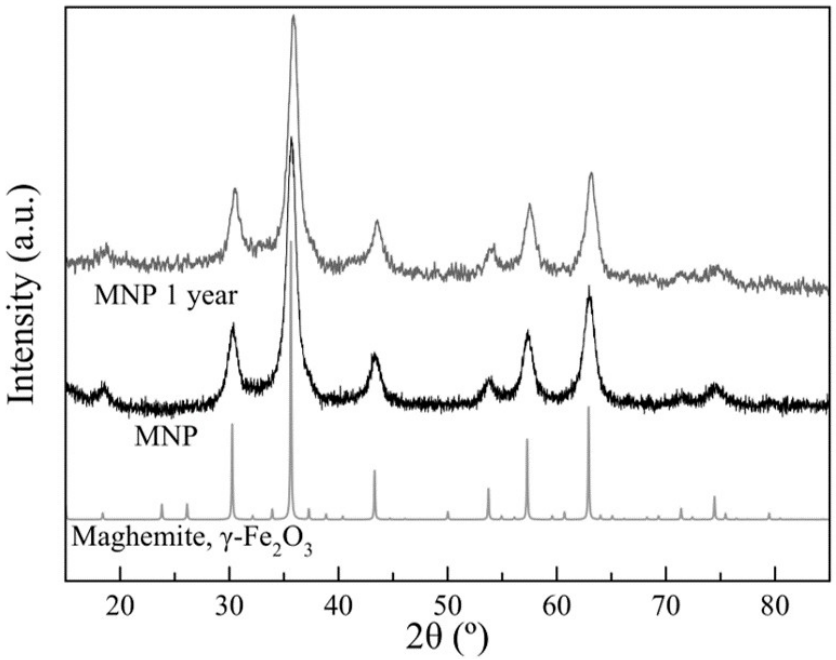

Figure SI2. XRD diffractograms of MNP immediately after synthesis (black line) and MNP one year after the synthesis (dark gray line) compared to a reference pattern of maghemite (light gray line).

TEM characterization of maghemite nanoparticles

Transmission electron microscopy (TEM) analyses were performed with a Tecnai G2 TEM (FEI) microscope operating at 200 kV. Colloids of maghemite nanoparticles were diluted and ultrasonicated in ultrapure water using an Allendale-Ultrasonic cleaner and then few droplets of the slurry were deposited on mesh copper TEM grids covered with thin amorphous carbon films and incubated for several minutes. A total of approximately 180 nanoparticles were manually measured using Image J software and the histogram obtained was fitted with a normal probability density function

DLS measurements

Dynamic light scattering (DLS) and Z potential measurements were performed in water on a Malvern Zetasizer Nano-ZS, using eleven (DLS) and twenty (Z potential) runs per measurement and three replicates at 25 °C.

XDR analysis of maghemite nanoparticles

Powder X-ray diffraction (PXRD) patterns of the samples were collected using a Bruker D8 Advance diffractometer equipped with a Lynx-eye position sensitive detector using Cu Kα radiation (λ = 1.54178 Å) generated at 40 kV and 40 mA. Diffractograms were recorded in the 2θ range from 15 to 85° with a step size (2θ) of 0.02 and a counting time of 1 s, and compared with maghemite crystallographic information file (CIF) from the American Mineralogist Crystal Structure Database (code_amcsd_0007898).

Stability of MNP colloid at low pH over time.

TEM, DLS and XDR assessment did not reveal relevant changes in morphology, size distribution, crystal structure and surface charge of maghemite nanoparticles in a colloid at pH 2.5 at least one year after synthesis (Figures SI1 and SI2).

3. AuNR characterization

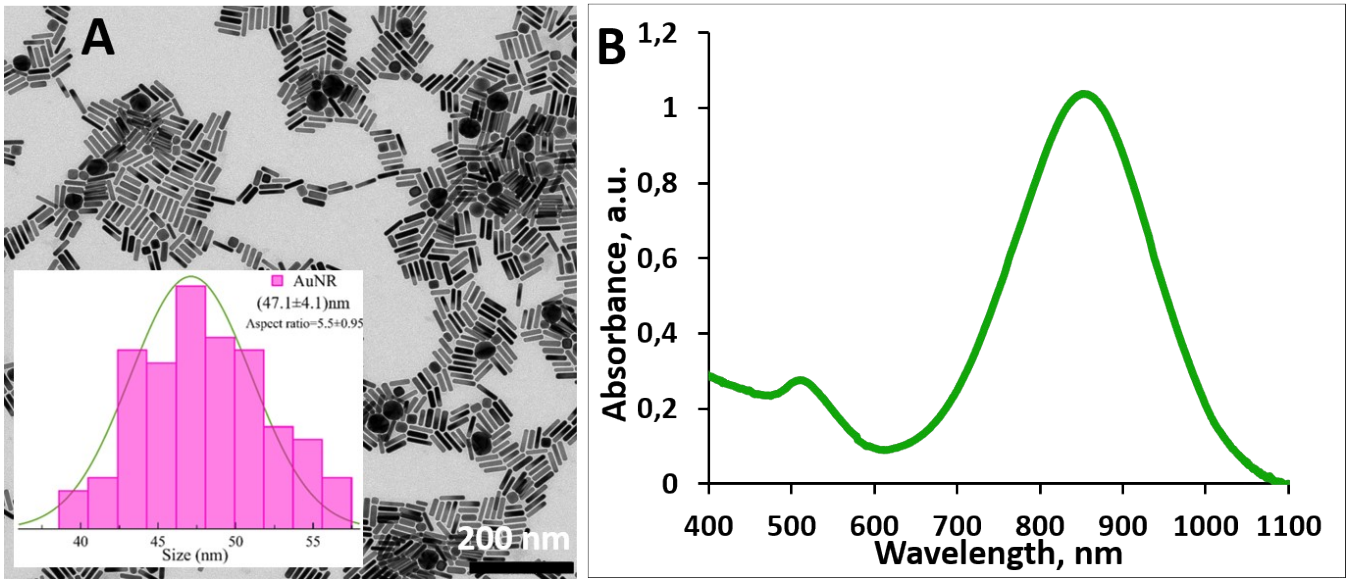

Figure SI3. A) TEM images of gold nanorods (AuNR) including an inset with the size distribution by TEM. Size of the nanoparticles was defined considering the length of the nanorods. The aspect ratio (length divided by width) is included in the inset. B) UV-vis spectra of AuNR-bacteria.

4. AuNPR characterization

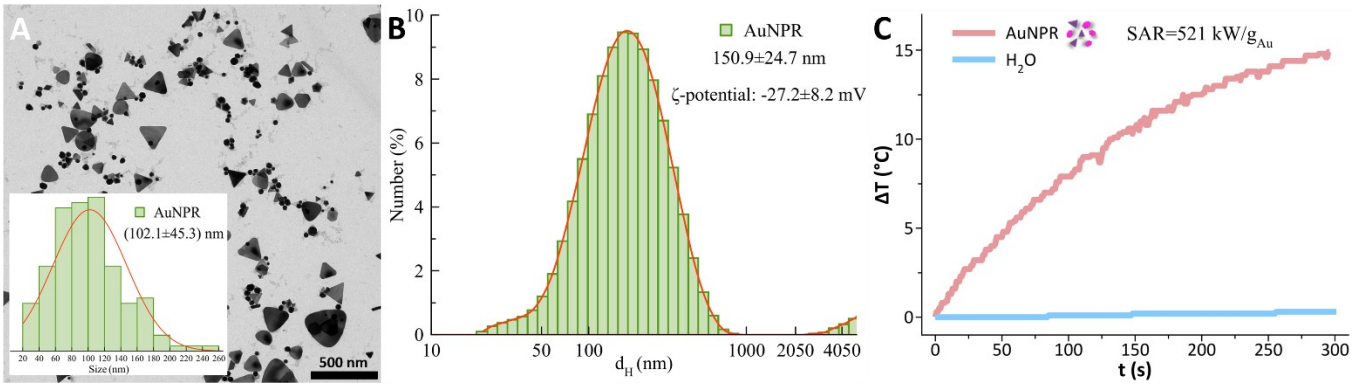

Figure SI4. A) TEM images of gold nanoprisms (AuNPR) including an inset with the size distribution by TEM. Size of the nanoparticles was defined considering the largest internal dimension of the nanoprism. B) DLS particle size distributions (hydrodynamic diameter, d_H) and ζ-potentials of AuNPR. C) Heating curves obtained after laser irradiation of 0.05 mg_{Au}/ml of AuNPR, plus water as a control sample (SAR value of AuNPR is included).

5. TEM and UV-vis study of AuNR-bacteria

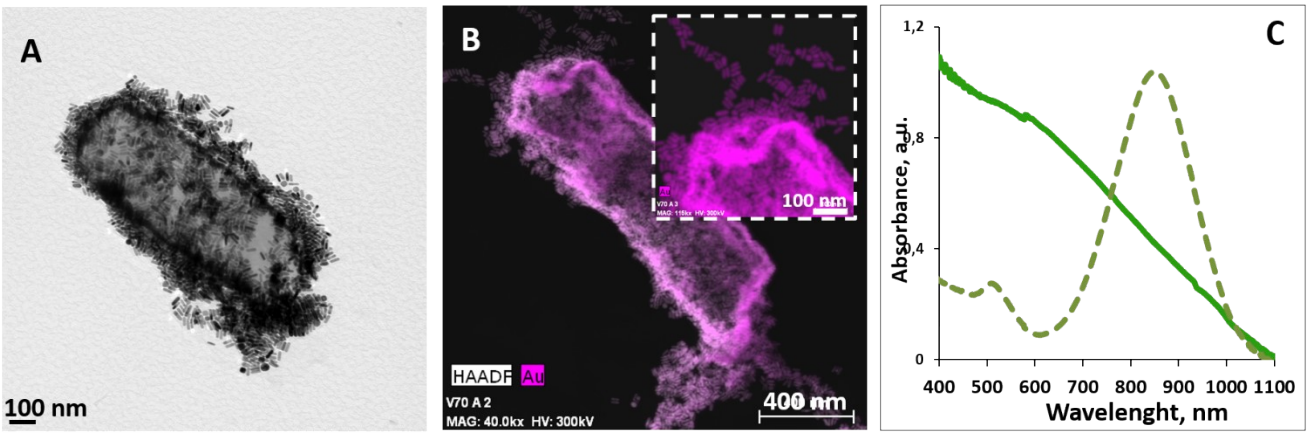

Figure SI5. A) TEM image of the AuNR-bacteria. B) HAADF-STEM combined with EDX compositional analysis of the AuNR-bacteria (gold in pink). C) UV-vis spectra of AuNRs (dashed line) and AuNR-bacteria (solid line).

6. Detailed TEM analysis of AuNPR-bacteria-EPS-MNP

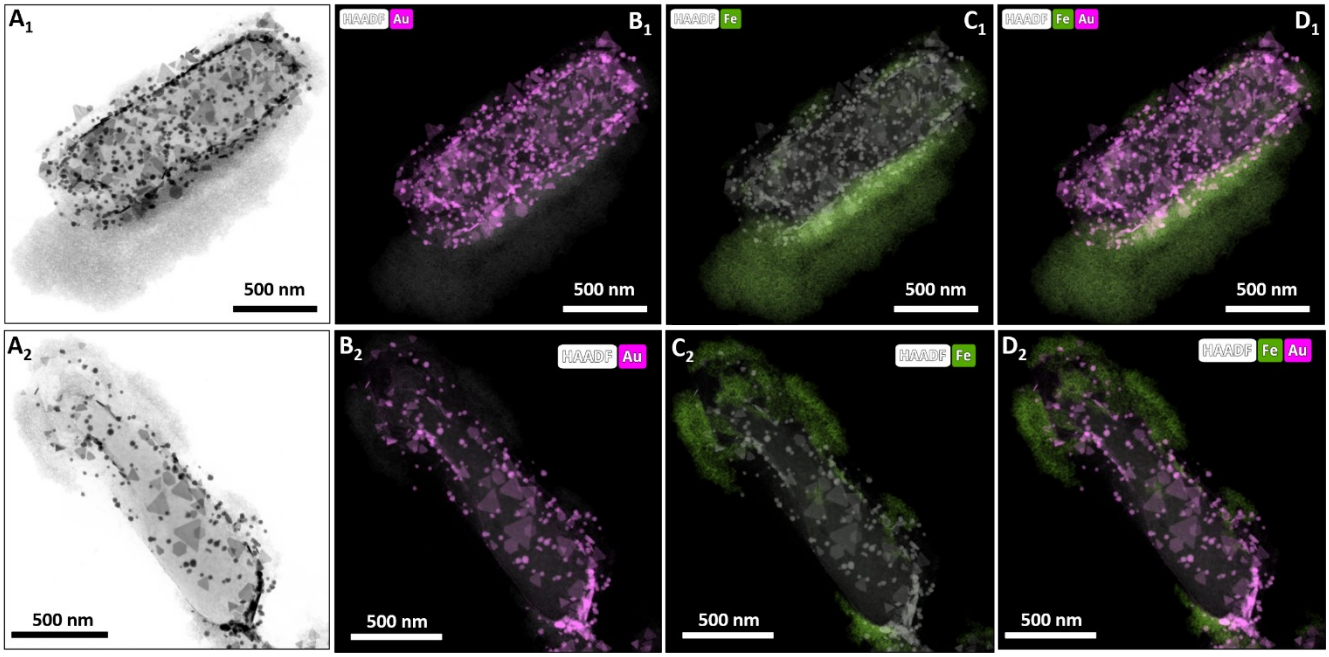

Figure SI6. A1 and A2) TEM image of AuNPR-bacteria-EPS-MNP. B1 and B2) HAADF-STEM combined with EDX compositional analysis images of AuNPR-bacteria-EPS-MNP (gold in pink).C1 and C2) HAADF-STEM combined with EDX compositional analysis images of AuNPR-bacteria-EPS-MNP (iron in green). D1 and D2) HAADF-STEM combined with EDX compositional analysis images of AuNPR-bacteria-EPS-MNP (iron in green and gold in pink)

7. UV-Vis spectrum of MNP-bacteria and their photothermal properties

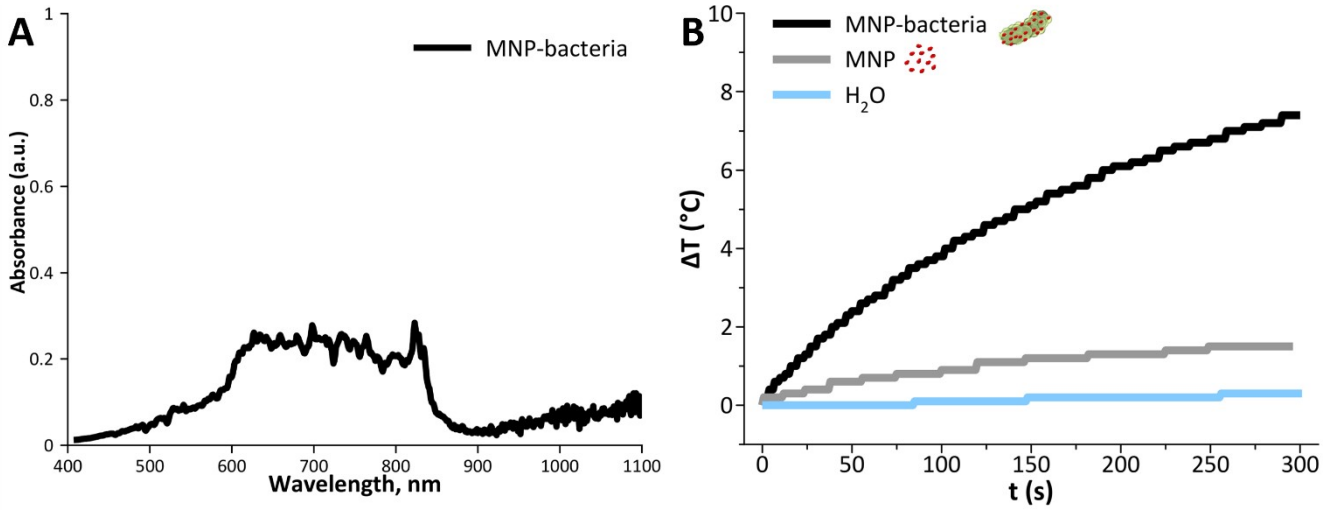

Figure SI7. A) UV-vis spectrum of MNP-bacteria revealed non-negligible absorptions at 1064 nm. B) Heating curves obtained after laser irradiation of MNP-bacteria (black line) and MNP (gray line), plus water as a control sample. Photothermal heating measurements were carried out at 0.5 mg_{Fe}/ml, the same concentration of iron that the magnetic hyperthermia measurements.

8. TEM study of aggregation of MNP

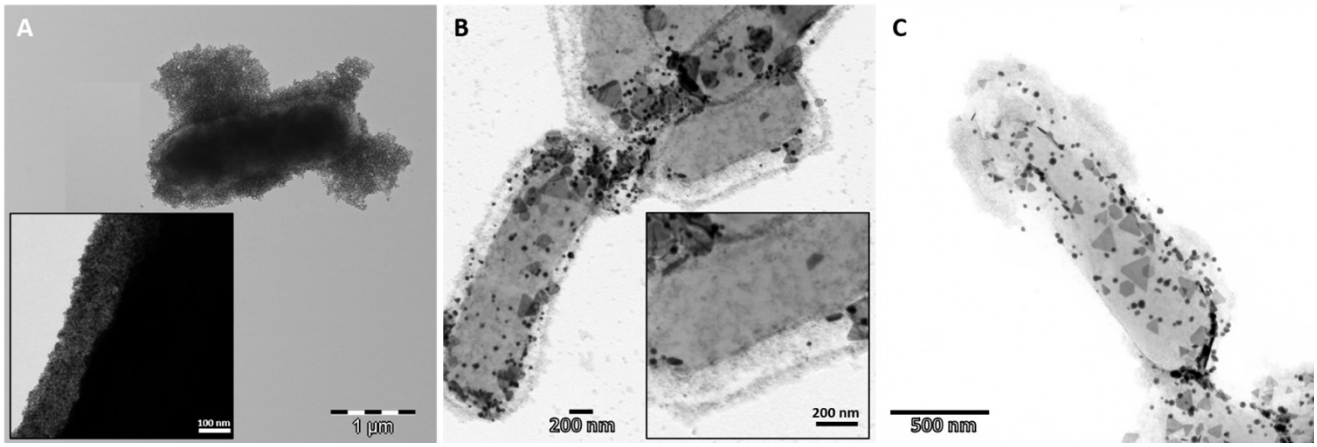

Figure SI8. TEM images of: A) MNP-bacteria, B) AuNPR+MNP-bacteria and C) AuNPR-bacteria-EPS-MNP showing different MNP aggregation patterns. Inset in A shows the greatest MNP aggregation of all samples.

9. Elemental composition of AuNP-MNP-bacteria

Sample	mg_{Au}/g_{sample}	mg_{Fe}/g_{sample}
AuNPR-bacteria	200±2.7	
AuNR-bacteria	30±0.4	
AuNPR+MNP-bacteria	165.5±2.3	257.3±3.3

AuNPR-bacteria-EPS-MNP	177.7±2.4	7.3±0.09
MNP-bacteria		179.3±2.3

Table SI1. Chemical analysis revealed the gold and iron concentration in each sample.